Impact of Reference Conditions on the Frequency Coupling Matrix of a Plug-in Electric Vehicle Charger

Joaquín E. Caicedo
Andrés A. Romero
Humberto C. Zini
Instituto de Energía Eléctrica
Univ. Nac. San Juan - CONICET
San Juan, Argentina
jcaicedo@iee.unsj.edu.ar

Roberto Langella
Dept. of Ind. and Inf. Eng.
The University of Campania
Aversa, Italy
roberto.langella@unicampania.it

Jan Meyer
Dept. of El. Eng. and Inform.
Techn. Universitaet Dresden
Dresden, Germany
jan.meyer@tu-dresden.de

Neville R. Watson
Dept. of Elect. and Comp. Eng.
University of Canterbury
Christchurch, New Zealand
neville.watson@canterbury.ac.nz

***Abstract*—Plug-in Electric Vehicles (PEVs) are progressively penetrating world markets. A significant impact on harmonic distortion in distribution networks is expected due to large-scale charging of PEVs at homes. Therefore, models that accurately predict the individual current injections are needed to perform harmonic studies, in particular frequency domain models such as those based on Frequency Coupling Matrices (FCM). In this paper, Fourier descriptors are used to estimate and compare the FCMs of a commercially available on-board PEV charger. Two models were calculated for two different supply reference conditions, namely, a sinusoidal voltage with no distortion, and a flat-top voltage. To that end, extensive laboratory measurements were carried out. Results show similar values in the parameterized admittances for both reference conditions. These results indicate a wide linear range in the coupled Norton model for this load, and should be probably attributable to the active power factor correction topology of the charger.**

***Index Terms*—Fourier descriptor, Frequency coupling matrix, Harmonic distortion, Plug-in electric vehicle, Power quality.**

I. Introduction

The current stock of Plug-in Electric Vehicles (PEVs) is over two millions worldwide, and it is expected to increase in forthcoming years [1], [2]. Most PEVs are expected to be charged at owners' homes [1], [3], hence, power quality and harmonic distortion in Low-Voltage (LV) networks will be affected. Several studies have demonstrated the growing harmonic distortion in LV networks due to PEV chargers, *e.g.* [4]–[7].

Harmonic studies for large-scale deployment of modern nonlinear loads, such as PEV battery chargers, are generally carried out in frequency-domain, due to computation advantages [8]. In most harmonic studies, PEV chargers have been modelled as constant current sources for each harmonic order [4]–[6]. However, more sophisticated models are needed when the supply voltage distortion is not negligible (as it is in LV networks), to obtain more accurate results [9], [10]. In that sense, the coupled Norton model allows for considering the harmonic interaction (between harmonic voltages and currents of different orders), hence, it improves the accuracy in the predicted injection of harmonic currents. To obtain the coupled Norton model, a linearization around an operating point of the nonlinear load is assumed [11]. Thereby, the model comprises a reference harmonic current and a Frequency Coupling Matrix (FCM) with the linear gradients that relate each harmonic current to the harmonic voltages [11]–[13]. This model is an approximation to the real behaviour of nonlinear loads, thus, the linear region around the operating point is limited, especially for highly nonlinear equipment and for current harmonic orders far from voltage harmonic orders [14]. Consequently, the parameters estimated for the Norton equivalent might depend on the supply reference voltage, which defines the operating point of the device. Most measurement-based methods to obtain the coupled Norton model of a device, assume a sinusoidal supply voltage (with no distortion) as reference [12]–[16]. However, the supply in public LV networks typically present a flat-top distortion, due to extensive connection of single-phase rectifier loads [17]. Therefore, an improvement of the model accuracy in simulations might be possible by selecting the reference supply closer to the typical flat-top voltage.

Coupled Norton models for PEV chargers have been developed to improve the accuracy in the predicted injection of harmonic currents [16]. Nonetheless, models in [16] neglect the phase angle dependency of the FCM. In this paper, the tensor parametrization [14], [18], [19], and the use of Fourier Descriptors (FDs) described in a companion paper [17], are implemented to estimate and compare the parameters of the coupled Norton model of a PEV battery charger, obtained for two reference conditions, namely, a sinusoidal voltage with no distortion, and a flat-top voltage. Besides, due to the tensor parametrization, the model also considers the phase angle dependency of the FCM.

Financial supports by the Consejo Nacional de Investigaciones Científicas y Técnicas (CONICET), the Deutscher Akademischer Austauschdienst (DAAD), and the Ministerio de Ciencia, Tecnología e Innovación Productiva (MINCyT), Argentina, under grant PICT 0388 – 2012, are gratefully acknowledged.

978-1-5386-0517-2/18/$31.00 ©2018 IEEE

II. Recalls on the Linearization of the Norton Equivalent Model

To better understand the linearization in the harmonic domain of a nonlinear load around an operating point, the linearization of a general nonlinear function is depicted in Figure 1. It is worth to note that the nonlinear function can be represented by the linear expression $y = ax + b$, for slight deviations Δx. Moreover, if a different operating point (x, y) is used as point of linearization, a change in the parameters of the linear expression (a, b) is expected.

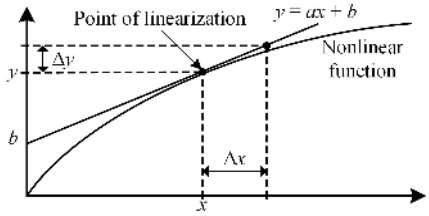

Figure 1. Linearization of a nonlinear function [17].

The compact expression of the Norton equivalent is presented in (1), where the FCM $\underline{\boldsymbol{Y}}$, and the reference current vector $\underline{\boldsymbol{I}}_{\text{ref}}$ represent the parameters of the linear expression (analogous to a, b), that is expected to change if a different operating point is used for linearization. Unlike the general linear expression, (1) is multivariate, and the number of variables depends on the harmonic orders to be considered.

$$\underline{\boldsymbol{I}} = \underline{\boldsymbol{Y}} \cdot \Delta\underline{\boldsymbol{V}} + \underline{\boldsymbol{I}}_{\text{ref}} \tag{1}$$

In this paper, the parameters $\underline{\boldsymbol{Y}}$ and $\underline{\boldsymbol{I}}_{\text{ref}}$ of a PEV charger are estimated and compared for two reference conditions.

III. Measurement Framework

A controlled voltage source generator with a 45 kVA amplifier was used to carry out the laboratory tests. The testbed setup is detailed in [20]. The measurement procedure was applied with two reference conditions, *i.e.*, fundamental voltage supply with no distortion (V_1 = 230 V), and voltage supply with a typical flat-top distortion derived from IEC 61000-4-13. The flat-top voltage waveform used for the tests is shown in Figure 2(a), and the corresponding harmonic spectrum is presented in Figure 2(b). The measurement procedure can be summarized as follows:

a) Supply the charger with the reference voltage, $\underline{\boldsymbol{V}}_{\text{ref}}$.
b) Compute the reference current in frequency-domain, $\underline{\boldsymbol{I}}_{\text{ref}}$.
c) Add a distorted voltage with third harmonic to the supply. *I.e.*, apply $\underline{\boldsymbol{V}}_{\text{ref}} + \Delta\underline{\boldsymbol{V}}$, where $\Delta\underline{\boldsymbol{V}}$ is an ideal sinusoidal signal with a magnitude of 1% of V_1, frequency equal to $3f_1$ and a phase angle equal to zero.
d) Compute the measured current $\underline{\boldsymbol{I}}$.
e) Estimate the values of $\underline{Y}_{h,3}$, by using (2).

$$\underline{Y}_{h,k} = \frac{\Delta\underline{I}_h}{\Delta\underline{V}_k} = \frac{\underline{I}_h - \underline{I}_{\text{ref-}h}}{\underline{V}_k - \underline{V}_{\text{ref-}k}} \tag{2}$$

f) Repeat steps c), d), and e), but varying the phase angle from 0 to 2π, in steps of π/6 rad.

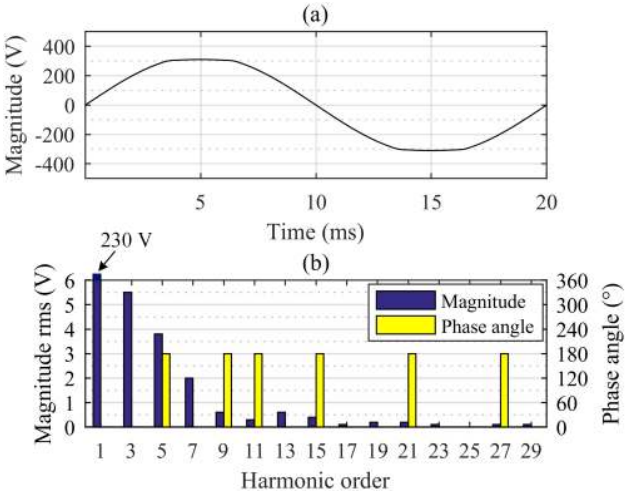

Figure 2. Flat-top voltage (a) waveform, and (b) harmonic spectrum.

g) Repeat steps c), d), e), and f), but varying the magnitude of the harmonic voltage in five steps until the maximum value established by the standard [21] is reached, for odd harmonic orders until the 7th (3rd: 5% of V_1; 5th: 6% of V_1; 7th: 5% of V_1), adding to $\underline{\boldsymbol{V}}_{\text{ref}}$ one harmonic at time.

Even harmonic orders are not considered in this analysis since these are usually negligible in the supply voltage distortion. For the sake of brevity, only harmonic orders until the 7th (the most significant in the charger) are analysed in this paper. Some aspects regarding accuracy of the estimated admittances are dealt in [12].

The background distortions applied in the tests are presented in Figure 3, exemplarily for the third harmonic voltage. Figure 3(a) shows a polar plot of the $\underline{V}_3$ locus, where the reference third harmonic voltage, $\underline{V}_{\text{ref-3}}$, is represented with an '*' symbol, in this case $\underline{V}_{\text{ref-3}}$ = 0 (located in the origin). Besides, the initial background distortion is marked with an 'o' symbol, for five different magnitudes of background distortion. As it is detailed in the companion paper [13], FDs allow for recognizing and classifying closed looped objects as it is the $\underline{V}_3$ locus in Figure 3(a). Thereby, for a perfectly accurate background distortion at sinusoidal reference, the magnitude $\underline{V}_k$ of the FD of order 1 is the only one expected to be different from zero. Its phase angle is expected to be exactly zero. For a different reference (*e.g.*, flat-top) the shift of the circle is represented by an additional FD component at order 0.

Figure 3(b) depicts the magnitudes of the $\underline{V}_3$ FDs. It can be verified that only the FD of order 1 is nonnegligible. However, the corresponding phase angle is not exactly zero (see Figure 3(c)), as the distortion generated by the amplifier has a slight phase angle offset. This slight phase shift should be considered when parameterizing the tensor admittances, in order to obtain accurate results [12]. Moreover, Figure 3(d) depicts the $\underline{V}_3$ locus, when the reference voltage is the flat-top waveform. It can be noted that $\underline{V}_{\text{ref-3}}$=5.5 V (see also Figure 2(b)). Consequently, not only the FD of order 1, but also the 0 FD is nonnegligible (see Figure 3(e)). Also in this case, the phase angle of the FD of order 1, observed in Figure 3(f) should be considered when computing the admittances.

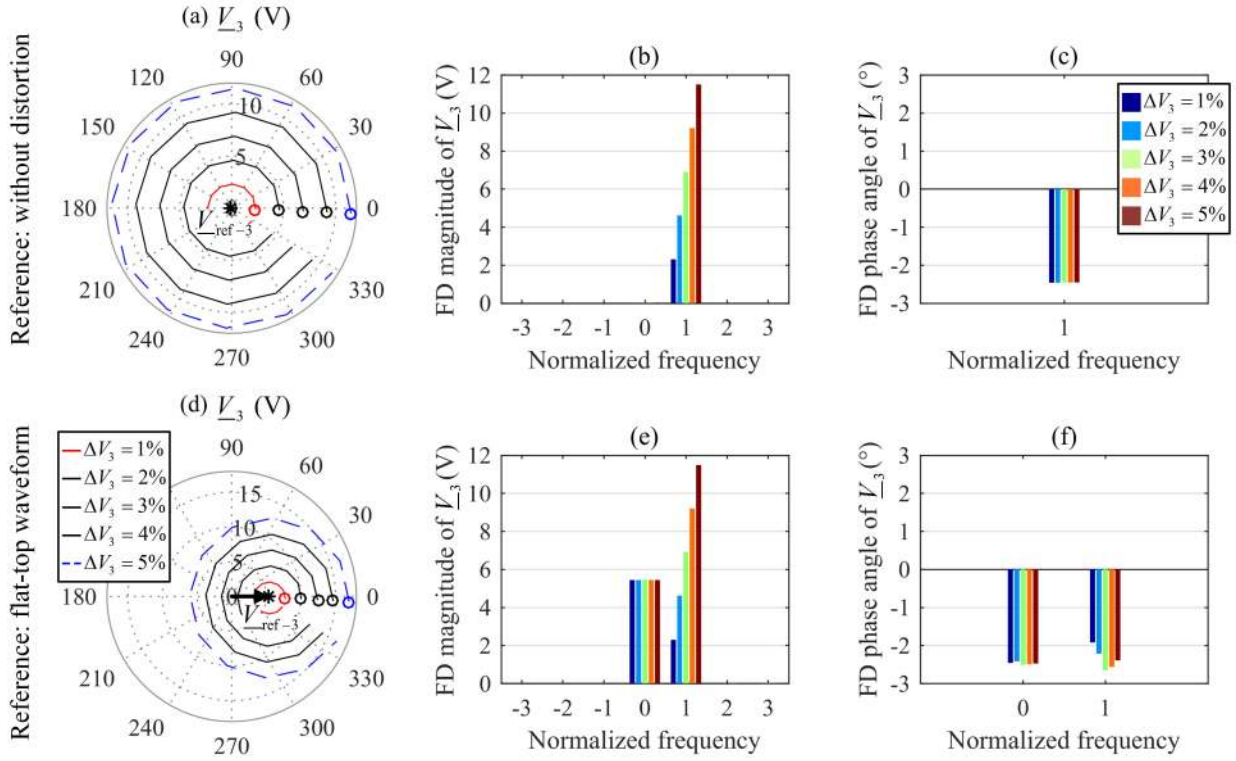

Figure 3. (a) Locus of $\underline{V}_3$ with the fundamental with no distortion as reference, and the corresponding (b) magnitude and (c) phase angle of the FDs. (d) Locus of $\underline{V}_3$ with the flat-top voltage waveform as reference, and the corresponding (e) magnitude and (f) phase angle of the FDs.

IV. Experimental Results

The loci of the third and fifth harmonic current contributions, $\Delta\underline{I}_3$ and $\Delta\underline{I}_5$, due to the third harmonic voltage $\Delta\underline{V}_3$, are depicted in the polar plots of Figure 4(a) and Figure 4(b). The loci of the corresponding estimated admittances, $\underline{Y}_{3,3}$ and $\underline{Y}_{5,3}$, are shown in Figure 4(c) and Figure 4(d). In this case, the reference condition is the fundamental voltage with no distortion. It can be noted that $\Delta\underline{I}_3$ describes circles in the complex plane. Consequently, the FDs of order 1 have the highest magnitudes (Figure 4(e)) demonstrating the almost perfect linear behaviour of the converter at this frequency and also the independence from the phase angle of the corresponding harmonic voltage. Furthermore, $\Delta\underline{I}_5$ describes ellipses in the complex plane and, therefore, the dominant orders of the FDs are the -1 and the 1. This can be verified in Figure 4(f) demonstrating that, again the relationship between current and voltage is linear but in this case the phase dependency has to be taken into account. Moreover, the locus of the admittance $\underline{Y}_{3,3}$ presents a significant offset from the origin, as can be confirmed with the dominant FDs of order 0 in Figure 4(g). This behaviour was also observed in other admittances that relate harmonic currents and voltages of the same order ($\underline{Y}_{5,5}$, $\underline{Y}_{7,7}$). The double circle described by the admittances can be better observed in $\underline{Y}_{5,3}$, where the dominant FDs are the orders -2 and 0 (see Figure 4(h)). A similar behaviour was noted in admittances that relate harmonics of different order ($\underline{Y}_{3,5}$, $\underline{Y}_{3,7}$, $\underline{Y}_{5,7}$, ...).

The loci for the same harmonic orders are presented in Figure 5, for a flat-top waveform as reference supply voltage. It is worth to note that the loci of $\Delta\underline{I}_3$, $\Delta\underline{I}_5$, $\underline{Y}_{3,3}$, and $\underline{Y}_{5,3}$ seem very similar for both reference conditions. Therefore, similar magnitudes of the FDs are also observed.

The companion paper [13] introduces two indices, which quantify the level of nonlinearity of harmonic current response (NLI_I) and calculated admittances (NLI_Y). The indices were computed for combinations of the 3rd, 5th, and 7th harmonic currents and voltages, for both reference supply voltages. Results are reported in Figure 6.

Similarly, as it was observed for different nonlinear loads in [13], the estimated NLI_I and NLI_Y values coincide in most cases, and for both reference supply voltages. On the other side, unlike results in [13], not only a direct relationship was observed between the indices and the background distortion magnitudes (*i.e.*, the more the voltage distortion, the more the NLI_I and NLI_Y values), but also an inverse relationship was observed in some harmonic orders (*e.g.*, for the variation of the third harmonic voltage, especially for the flat-top reference supply voltage). Furthermore, similar levels of nonlinearity and trends are noted for both reference supply voltages. The highest difference in the levels of nonlinearity occurs, in most of the analysed cases, in the smallest values of background distortion ΔV_k (*e.g.*, in the nonlinearity indices estimated for h=5, k=3). Moreover, the level of nonlinearity is slightly higher for the flat-top reference voltage in most cases. It is also worth to note that the diagonal indices (*i.e.*, interaction of harmonic currents and voltages of the same order, h=k) present smaller values than off-diagonal indices.

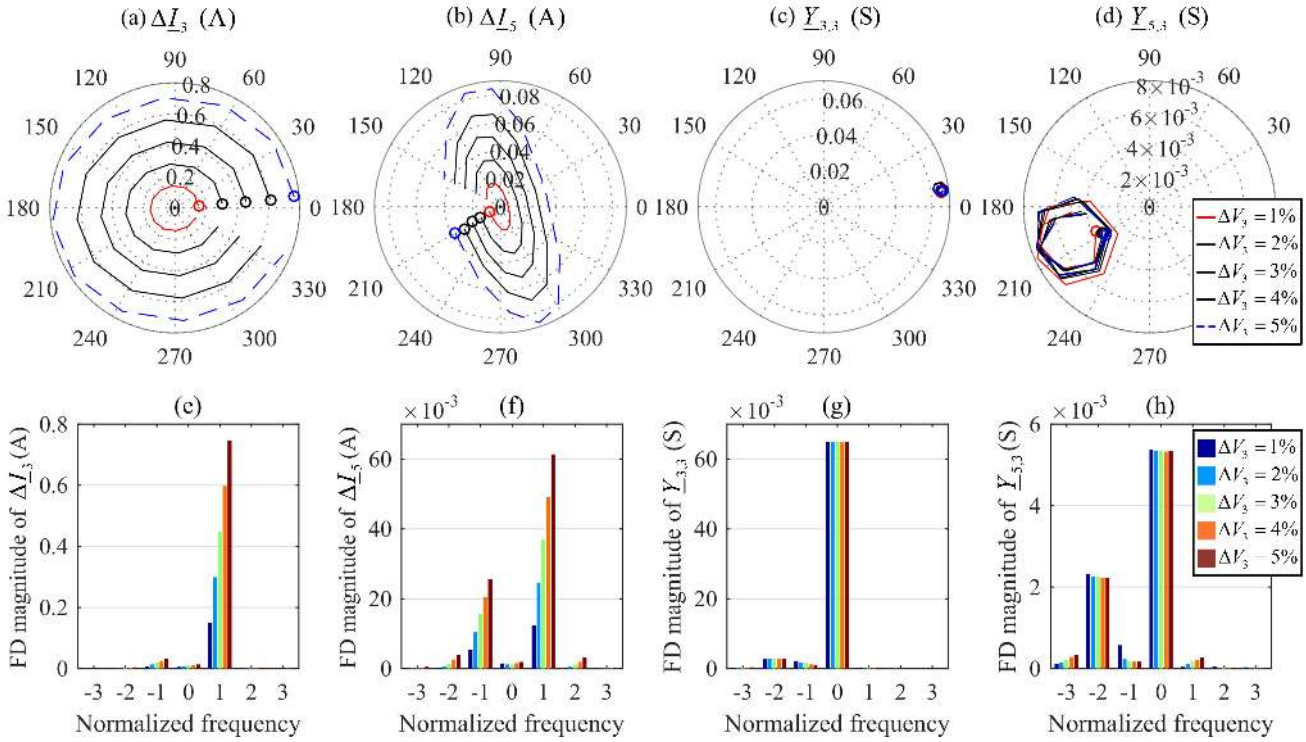

Figure 4. Reference supply voltage: fundamental with no distortion. Loci of: (a) the contributions $\Delta\underline{I}_3$, and (b) $\Delta\underline{I}_5$ caused by the distortion $\Delta\underline{V}_3$; the estimated admittances (c) $\underline{Y}_{3,3}$, and (d) $\underline{Y}_{5,3}$. Corresponding magnitudes of the FDs of (e) $\Delta\underline{I}_3$, (f) $\Delta\underline{I}_5$, (g) $\underline{Y}_{3,3}$, and (h) $\underline{Y}_{5,3}$.

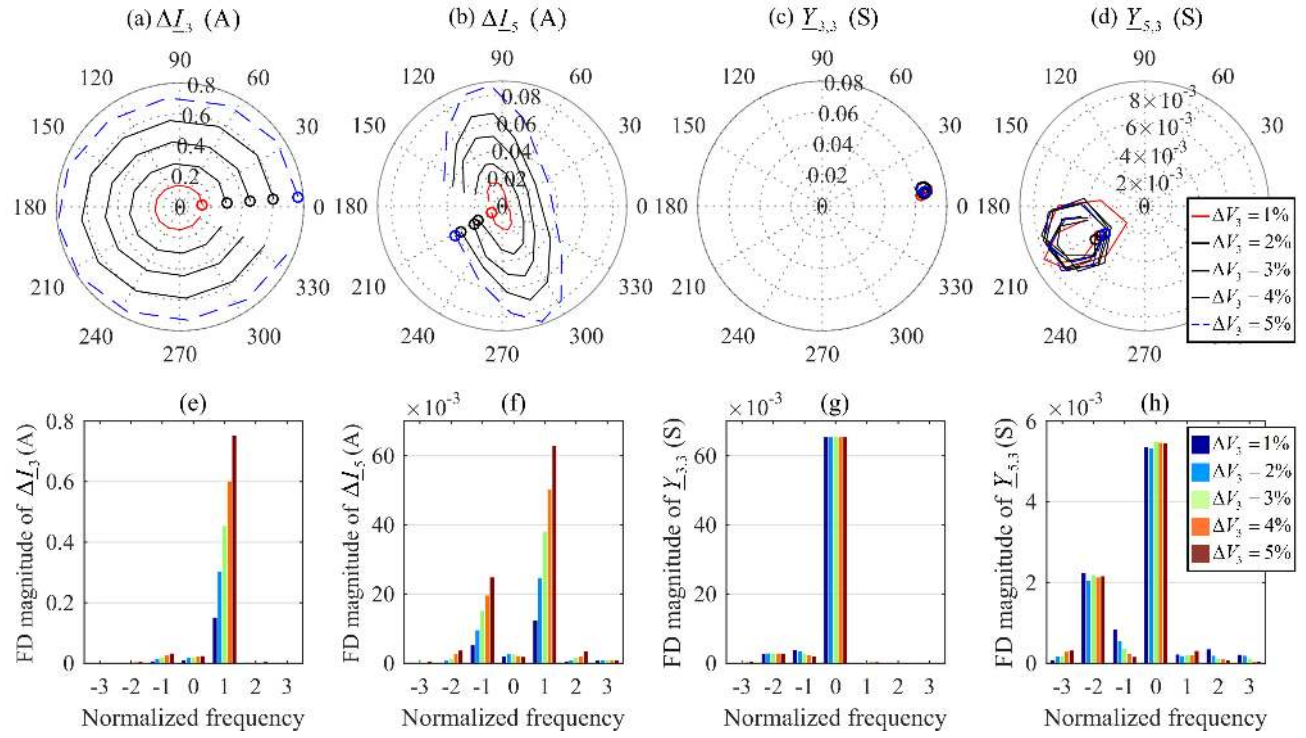

Figure 5. Reference supply voltage: flat-top. Loci of: (a) the contributions $\Delta\underline{I}_3$, and (b) $\Delta\underline{I}_5$ caused by the distortion $\Delta\underline{V}_3$; the estimated admittances (c) $\underline{Y}_{3,3}$, and (d) $\underline{Y}_{5,3}$. Corresponding magnitudes of the FDs of (e) $\Delta\underline{I}_3$, (f) $\Delta\underline{I}_5$, (g) $\underline{Y}_{3,3}$, and (h) $\underline{Y}_{5,3}$.

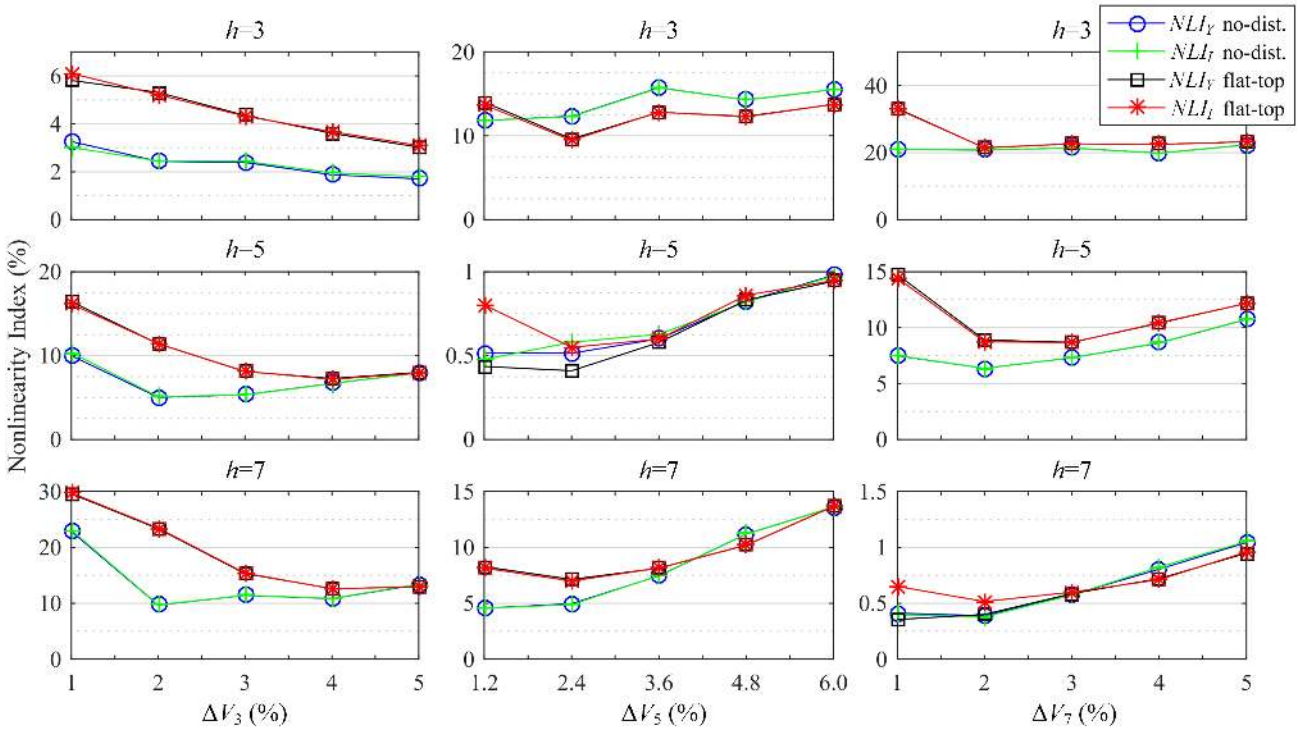

Figure 6. Estimated nonlinearity indices NLI_Y and NLI_I for different levels of background distortion; two reference conditions: fundamental voltage with no distortion (no-dist.), and flat-top voltage waveform (flat-top); and the combinations of voltage and current harmonic orders 3, 5, and 7.

V. Comparison of the Norton Equivalent Models

A coupled Norton model was obtained for the PEV charger, for each reference supply voltage (*i.e.*, no distortion and flat-top). The FCM for each reference condition is shown in the intensity graphs of Figure 7.

Note that the FCMs are parameterized, hence, each admittance $\underline{Y}_{h,k}$ is represented by a rank-2 real-valued tensor

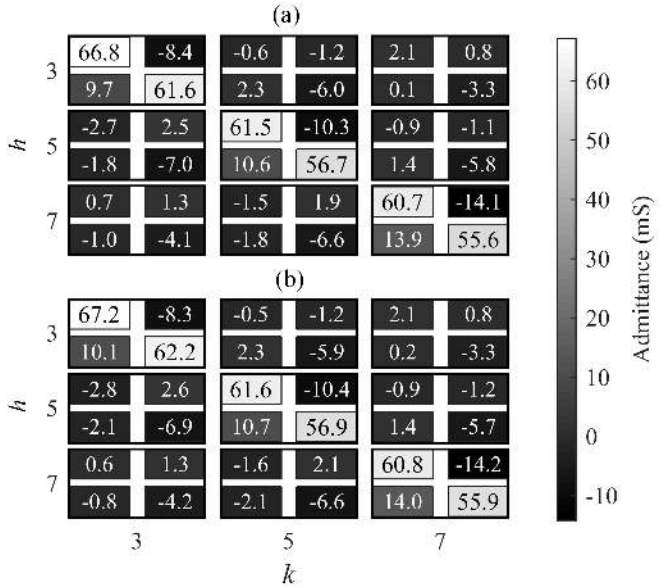

Figure 7. Parameterized FCM of the PEV charger, considering the 3rd, 5th and 7th harmonic orders, for the reference conditions: (a) fundamental with no distortion, and (b) flat-top voltage.

matrix (see Section III of [13]). Diagonal elements of the FCM have much higher magnitudes than off-diagonal elements. This is expected for nonlinear loads with active Power Factor Correction (PFC), such as PEV chargers. It can be observed that values of both matrices are very similar, especially in diagonal elements.

The absolute difference between the corresponding elements of the FCMs was quantified by computing (3). Results for the elements of the FCMs are presented in the intensity graph of Figure 8.

$$\Delta y_{\text{no-dist, flat-top}} = y_{\text{flat-top}} - y_{\text{no-dist}} \tag{3}$$

Figure 8 demonstrates the similarity in both FCMs. Thereby, for the studied PEV charger the reference condition for obtaining the FCM has a minor influence. This is also suggested by the nonlinearity indices, which are rather low and confirm that for the considered harmonics, especially

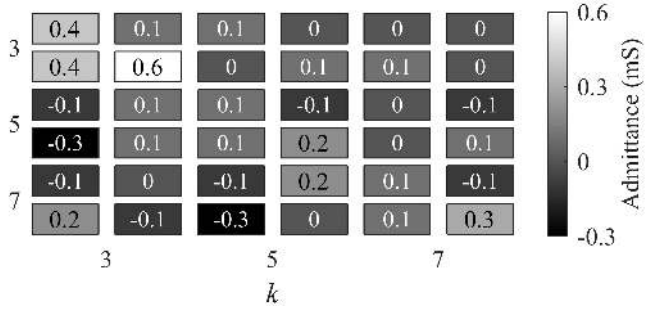

Figure 8. Difference of the FCM obtained with the flat-top reference voltage, from the FCM obtained with the fundamental with no distortion as reference.

those of same order, the charger behaves rather linear.

In a similar fashion, Table I reports the measured reference harmonic currents, $\underline{\boldsymbol{I}}_{\text{no-dist}}$ and $\underline{\boldsymbol{I}}_{\text{flat-top}}$, for the two reference supply voltages: no distortion and flat-top, respectively. Besides, the absolute difference and the relative difference of the magnitudes between both, were computed by using (4) and (5).

$$\Delta \boldsymbol{I}_{\text{no-dist, flat-top}} = \underline{\boldsymbol{I}}_{\text{flat-top}} - \underline{\boldsymbol{I}}_{\text{no-dist}} \tag{4}$$

$$\delta \boldsymbol{I}_{\text{no-dist, flat-top}} = \frac{\left|\underline{\boldsymbol{I}}_{\text{flat-top}}\right| - \left|\underline{\boldsymbol{I}}_{\text{no-dist}}\right|}{\left|\underline{\boldsymbol{I}}_{\text{no-dist}}\right|} \times 100\% \tag{5}$$

TABLE I. COMPARISON OF THE REFERENCE HARMONIC CURRENTS FOR TWO REFERENCE SUPPLY VOLTAGES (NO DISTORTION AND FLAT-TOP)

h	$\underline{\boldsymbol{I}}_{\text{no-dist}}$ (mA)	$\underline{\boldsymbol{I}}_{\text{flat-top}}$ (mA)	$\Delta \boldsymbol{I}_{\text{no-dist, flat-top}}$ (mA)	$\delta \boldsymbol{I}_{\text{no-dist, flat-top}}$ (%)
3	–855 – j407	–506 – j405	–349 – j2	32
5	–169 – j46	–427 – j76	258 + j30	–148
7	–150 – j26	–17 – j9	–133 – j17	87

Unlike the FCM $\underline{\boldsymbol{Y}}$, the reference current $\underline{\boldsymbol{I}}_{\text{ref}}$ present a significant change in the analysed harmonics, according to Table I, as expected.

VI. CONCLUSIONS

The impact of the supply voltage reference conditions on the measurement-based identification of the coupled Norton parameters for an on-board PEV charger was analysed. It has been shown that the FCM, which represents the part of the model depending on voltage harmonics, exhibits only a slight change. This suggests a large enough linearity range to overlap between sinusoidal reference supply voltage with no distortion (laboratory) and flat-top reference conditions as usually found in public LV networks. Furthermore, the estimated nonlinearity indices for the analysed harmonic orders, NLI_I and NLI_Y, suggest that the harmonic admittances, $\underline{Y}_{h,k}$, for current and voltage harmonics of the same order (diagonal of the FCM), are mainly determined by the grid side filter circuit of the charger (behave rather linear). Besides, off-diagonal elements of the FCM are mainly caused by nonlinear effects like control of the charger.

As most PEV chargers use similar circuit topologies, namely, rectifier with active PFC, it is very likely that findings of this study also apply to the majority of PEV chargers. Consequently, the use of a sinusoidal supply voltage as reference for the identification of the Norton equivalent parameters is justified. Further similar studies should be carry out for devices with different topologies, *e.g.* with no PFC and passive PFC circuits.

REFERENCES

[1] International Energy Agency, "Global EV Outlook." 2017.

[2] J. Brady and M. O'Mahony, "Development of a driving cycle to evaluate the energy economy of electric vehicles in urban areas," *Appl. Energy*, vol. 177, 2016.

[3] S. Speidel and T. Bräunl, "Driving and charging patterns of electric vehicles for energy usage," *Renew. Sustain. Energy Rev.*, vol. 40, 2014.

[4] C. Jiang, R. Torquato, D. Salles, and W. Xu, "Method to assess the power-quality impact of plug-in electric vehicles," *IEEE Trans. Power Deliv.*, vol. 29, no. 2, pp. 958–965, 2014.

[5] H. Sharma, M. Rylander, and D. Dorr, "Grid impacts due to increased penetration of newer harmonic sources," *IEEE Trans. Ind. Appl.*, vol. 52, no. 1, 2016.

[6] A. Aljanad and A. Mohamed, "Harmonic Impact of Plug-In Hybrid Electric Vehicle on Electric Distribution System," *Model. Simul. Eng.*, vol. 2016, 2016.

[7] S. Müller, F. Möller, M. Klatt, J. Meyer, and P. Schegner, "Impact of Large-Scale Integration of E-Mobility and Photovoltaics on Power Quality in Low Voltage Networks," in *ETG Kongress*, 2017.

[8] A. Medina, J. Segundo, P. Ribeiro, W. Xu, K. L. Lian, G. W. Chang, V. Dinavahi, and N. R. Watson, "Harmonic analysis in frequency and time domain," *IEEE Trans. Power Deliv.*, vol. 28, no. 3, pp. 1813–1821, 2013.

[9] A. Mansoor, W. M. Grady, A. H. Chowdhury, and M. J. Samotyj, "An Investigation of Harmonics Attenuation and Diversity Among Distributed Single-Phase Power Electronic Loads," *IEEE Trans. Power Deliv.*, vol. 10, no. 1, pp. 467–473, 1995.

[10] J. E. Caicedo, A. A. Romero, and H. C. Zini, "Assessment of the harmonic distortion in residential distribution networks: literature review," *Ing. e Investig.*, vol. 37, no. 3, pp. 72–84, 2017.

[11] J. Arrillaga, A. Medina, M. L. V. Lisboa, P. Sánchez, and M. A. Cavia, "The harmonic domain. a frame of reference for power system harmonic analysis," *IEEE Trans. Power Syst.*, vol. 10, no. 1, 1995.

[12] D. Gallo, C. Landi, R. Langella, M. Luiso, A. Testa, and N. Watson, "On the Measurement of Power Electronic Devices' Frequency Coupling Admittance," in *2017 IEEE International Workshop on Applied Measurements for Power Systems (AMPS)*, 2017, pp. 1–6.

[13] R. Langella, J. E. Caicedo, A. A. Romero, H. C. Zini, J. Meyer, and N. R. Watson, "On the Use of Fourier Descriptors for the Assessment of Frequency Coupling Matrices of Power Electronic Devices," *submitted to the 18th International Conference on Harmonics and Quality of Power, ICHQP*. Ljubljana, Slovenia, 2018.

[14] J. E. Caicedo, A. A. Romero, and H. C. Zini, "Frequency domain modeling of nonlinear loads, considering harmonic interaction," in *2017 3rd IEEE Workshop on Power Electronics and Power Quality Applications, PEPQA 2017 - Proceedings*, 2017.

[15] M. Fauri, "Harmonic modelling of non-linear load by means of crossed frequency admittance matrix," *IEEE Trans. Power Syst.*, vol. 12, no. 4, pp. 1632–1638, 1997.

[16] S. Müller, J. Meyer, P. Schegner, and S. Djokic, "Harmonic modeling of electric vehicle chargers in frequency domain," in *Int. Conf. Renew. energies and Power Quality (ICREPQ)*, 2015, pp. 1–6.

[17] L. Frater, "Light flicker and harmonic modelling of electrical lighting," Ph.D. dissertation. University of Canterbury, 2015.

[18] B. C. Smith, N. R. Watson, A. R. Wood, and J. Arrillaga, "Harmonic tensor linearisation of HVdc converters," *IEEE Trans. Power Deliv.*, vol. 13, no. 4, pp. 1244–1250, 1998.

[19] J. Arrillaga, B. C. Smith, N. R. Watson, and A. R. Wood, *Power system harmonic analysis*. John Wiley & Sons, 1997.

[20] F. Möller, J. Meyer, and P. Schegner, "Load model of electric vehicles chargers for load flow and unbalance studies," in *9th International: 2014 Electric Power Quality and Supply Reliability Conference, PQ 2014 - Proceedings*, 2014.

[21] EN 50160, "Voltage characteristics of public distribution systems," 2010.